Journal of Green Engineering (JGE)

Volume-10, Issue-2, February 2020

A Grey Wolf Optimization Based MPPT Algorithm for Energy Harvesting PV System

[1]Rana Adil Abdul-Nabe, [2]Rawaa A. Abdul –Nabi, [3]Sara Al-waisawy

[1]Al - Mussaib Technical Institute /Al- Furat Al - Awsat Technical University ,Babylon, Iraq.E-mail: ranaalbakri2018 @gmail.com
[2]AL-Mussaib Technical College, AL-Furat Al-Awsat Technical University, Babylon, Iraq.E-mail: com.aa.rwaa@atu.edu.iq,
[3]AL-Mussaib Technical College, AL-Furat Al-Awsat Technical University, Babylon, Iraq. E-mail:com.ks.sara@atu.edu.iq

Abstract

Solar photovoltaic array-based energy generation is now receiving more attention to supplying multiple loads such as water pumps. Agricultural, household and industrial water supply irrigation is aimed by photovoltaic array water pumping scheme. In proposed system, MPPT technique with solar PV system is used GWO optimization algorithm. Lue converter provides LDC motor soft starting with necessary control. BLDCM speed can be limited with the help of VSI which is fed with BLDCM. Between the VSI and the solar array the converter is acts as interface and its feds the BLDC motor.

Keywords: SPV array, Luo Converter, BLDC motor, Centrifugal water pump, Grey Wolf Optimization.

1 Introduction

Various algorithms deal to photovoltaic system fed BLDC motor using PI controller. In photovoltaic systems, an important role is played by MPPT controllers. The highest power of operating the solar PV arrays used so that it is ability of VSI.

Journal of Green Engineering, Vol. 10_2, 299–326. Alpha Publishers

Alpha Publishers

The proposed MPP tracker is used to achieve the target within high convergence rate as compared to the conventional MPPT. The controller which is being proposed is related and examined the function of popular conventional technique with different conditions [1]. The proposed PV system is modelled with the help of MATLAB 2016a software. From result, MPP can be track quickly (less than 0.3 seconds) while comparing existing techniques. The existing system takes greater than 10 seconds in computation time. Computation time is high by using MPP under partial shading condition. In North America the energy cost is compensated due to low water flow. BLDC is designed with minimal pulsating torque [2]. The new controller is created on an adapted field concerned with control. The PCB controller is of double layers to propose a less expensive result. It was developed under best efficiency (98.2%) with the algorithm plotting the yield properties (Head, Flow) to the provided properties (speed, torque).

Two MPPT methods, P&O and IC are done by MATLAB a for transferring extreme power. The outcomes approve that under shady climate conditions, the presentation of the steady conductance calculation displays marginally higher proficiency than simulation of the perturb and watch calculation [3]. The framework with MPPT use over 96% of electric vitality that are delivered from photovoltaic generator and, then again, another framework provides the accuracy of 34.9%.

This MPPT methods reflects their aptness in systems which involvement a large range of working circumstances. The choice of MPPT is highly application-dependent, from this, unmistakably each MPPT technique has its own preferences and drawbacks. The goal is to decrease the restitution time, when utilizing sunlight-based boards in private areas. The extreme power can be calculated along these lines. It should be noted that the ripple, this ripple minimization is some difficult in MPPT [4]. Therefore, incremental conductance and remark and perturbation algorithms are phase of dual varying techniques suitable. By mimicking an independent photovoltaic system, these two techniques have been assessed to associate the photovoltaic panel to the heap. Over a wide scope of various light conditions, specifically, the capacity of every technique has been considered. Over a wide scope of illumination settings and burden profiles, the yield Results demonstrate that the improve of irritate and watch calculation displays brisk powerful execution and accomplishes steady state level superior to the gradual conductance strategy [5]. The irradiance value can be change with respect to time. In one second section reading is obtained, but two seconds it can be increased up to 1000 w/m^2

Different sustainable power sources are used. Solar PV system can be widely used, because the cost is less while comparing other PV systems. To remove the most extreme power, MPPT are utilized photovoltaic, fluffy with MPPT strategy is noticed to give better outcomes to haphazardly

differing air conditions on contrasting with different techniques [6]. For more years, Induction Motors were being used and at present supplanted using Brushless DC Motors on account of their focal points. Being a peak effectiveness and silent process are the main advantages. MPPT with septic convertor to determine the peak power from the photovoltaic module of the fuzzy system. Associating to various BB converters like fly back, the Sepik converters can take off large power [7]. The Hall Effect sensors produces a switching signal, the BLDC can be act as a Voltage source Inverter. Still constant speed motor can act as the current simulated system. For applications, for example, pumping, grinding and so on., the main method of driving remote territories can be accomplished by sun-oriented power, Therefore, rather than utilizing Induction motor inferable from their misfortunes, it is smarter to utilize a BLDC motor.

Based on a hereditary assisted, multilayer perceptron NN structure, the MPPT controller is created. The concealed layer, hereditary assistance in the NN is utilized. GA-LM techniques is applied only in training the network [8]. Also, by using MPPT controller, extended scheduling of operation can be performed. The proposed system gives rise to best way to manage energy using such techniques in photovoltaic systems analyzed in rural places that can be concluded from the results.

The proposed a standalone solar photovoltaic powered air-cooling system constitutes of DC to DC boost circuit, centrifugal water pump, fan and brushless motors. These are connected from two voltage source inverters. Based on Silver Mean Method, a simple and efficient MPPT technique is utilized here. P and O performance can be calculated with MPPT and the output parameters are analyzed [9]. With the original features of projected system include appropriate design of SPV array, a new SMM based MPPT controller with boost converter, the performance analysis has demonstrated. The results of simulation show superior outputs and regardless of the environmental conditions [10].

For satisfying human needs, water resources are vital. However, physically water is rare, there are areas. There are people with water shortage problem are face in about One quarter of global population. To stream water pump using Brushless DC motor, photovoltaic system is the core power producer. There are three control units in proposed control strategy. The first unit controls the speed and hysteresis current manager for B BLDCM. The control unit used the second time is tracked for the MPP, and third controller controls the battery charging and discharging system [11].

As a result, it concludes that an efficient study is necessary to design PGS since each of these approaches possess both advantages and disadvantages. This paper reviews the four groups of algorithms named as optimized MPPT, hybrid MPPT, designing approaches, and different

converter topology. In addition, this method also suggests to perform an efficient research in future for the partial shaded PV systems [12].

Tracking time and oscillation drawbacks present around Maximum power point. To generate the matching ratio fed to a (PI/PID) controller. Under certain circumstance,the gains of Proportional Integral Derivative controller are calculated and actual value is maintained as additional operating conditions too, under varying some conditions doesn't provide exact result from the loop of the system [13]. Here without using any additional sensors introduced, which is used to determine the gain value. In this way to obtain the MPPT irradiance value is 99.73%.

For accomplishing a natural double voltage and power stream control, the three Port Converter was used and worked in unidirectional as well as bidirectional way and makes the framework more practical by all the while Switch check. By controlling torque swell during segment to part substitutions of BLDC engine, another technique for torque control has been used [14]. The three-port converter is utilized for accomplishing a characteristic double voltage and power stream control. For speed control of BLDC engine without relentless state blunder, a palatable shut circle execution has been accomplished. With immaterial motions around ideal working point is accomplished. Ideally choosing the underlying estimation of obligation proportion and its bother size offers delicate turning over of BLDC engine by gradually expanding. Solar PV system can be used for energy reproduction in battery. Initially the time duration varies from 0 to 0.39 seconds. This particular time the solar energy can be separated in the range of (200 W/m2), after that calculated the irradiance value from the solar system of time duration at 0.4 second [15].

The phase current sensors are for achieving a controlling operation. This leads to amplified price, dimensions, complication of the circuit and efficiency of the motor is very less. This project is solar photovoltaic system it will be converted solar energy to electric energy conversion system via water pump [16]. The speed controlling system is not used, so that the system provides higher efficiency in slow speed. But the complexity of the system is high, due to complexity additional circuits are linked with it. Brushless DC motor provides the equal amount of water supply at slow speed conditions. The phase current sensor is the costly product in this system. The replacement of this sensor, the entire circuit cost is very less. The photovoltaic array power is optimized successfully under some conditions. For controlling irradiance, the duty cycle can be introduced in each irradiance level. In this system irradiance value is 1000W/m2 to 500W/m2. The duty cycle can be depending on the controlling speed of the system.

It delivers maximum energy as probable. Two different MPPT algorithms is being introduced. The pulse width modulation algorithm has been added with the motor for controlling the speed and simulated result

from the loop of the system. Combination of two BLDC motor is implemented for tracing the maximum power of the solar system A comprehensive comparative between PO MPPT and IC MPPT are obtained and discussed [14]. At lower values of irradiance 200W/m2 the efficiencies are 92% for PO MPPT and 96% for Improving conductance MPPT because doesn't oscillate as much as P&O toward the MPP and intending to resolve the problem.

The only advantage is there is reduction in efficiency but otherwise all other are defects which include amplified cost, dimensions, and complexity. The system is worked with a collective VSI loop, BLDC motor reach the stable state and the speed of the motor is 1745 rpm [12]. A DC-DC converter provides the better result in brushless motor by using water pumping techniques. Furthermore, sensors are used to calculate the phase current and to eliminate this current.

The proposed research is organized as follows: Section 2 presents the block diagram of the proposed system with explanations and section 3 gives a detailed study about the design flow of BLDC motor, photovoltaic array and centrifugal water pump. Grey Wolf Optimization (GWO) algorithm is explained in section 4. Section 5 introduces the simulation results performed using MATLAB/SIMULINK along with relevant discussions. Section 6 describes the conclusion and future work.

2 Proposed System

The proposed system has been shown in figure 1. It consists of SPV array, Luo converter; three phase VSI, GWO and centrifugal pump.

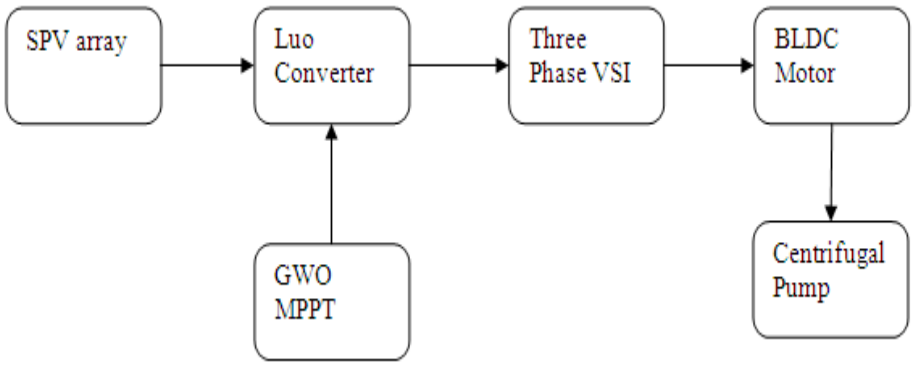

Figure 1 Block diagram of the proposed system

2.1 Photovoltic Array

Combination of solar sell is formed the PV array of the module. In uniform solar isolation the array output power equals the all cells output power. The performance is affected if the cells are not equally illuminated, in a series PV module. The shadows from a neighbor's houses, trees, or even a shadow of one solar array to the other one, are the causes of non-uniform isolation. Because of shading, almost 80% power losses is recorded.

Partial shading is the condition when the components linked in series and parallel and result is the power generation by the various modules that are different for the same panel rating, when it doesn't receive same illumination as compared to the other modules.

The efficiency of a solar cell becomes less so that the efficiency is also not increased. The maximum power transfer theorem is to calculate the PV panel efficiency. MPPT efficiency is expressed in the below equation.

$$\eta = \frac{\int_0^t \text{Pmeasured(t)dt}}{\int_0^t \text{Pactual(t)dt}} \quad (1)$$

In grid connected PV method, MPPT is now familiar and it is more prominent, and V-I characteristics is nonlinear. So, for a certain load, it is very challenging to produce a constant power. Most of the people consider grid connected PV system as a mechanical device. This device is used for tracing the sun radiation and automatically tilts the panel in the direction of solar radiation side. So, it tracks more power speedily. MPPT is also well-known as electronic device, which extracts highest available system power. In this way to compare the impedance of load with PV cells, the panel's electrical operating point and duty cycle are varied. These two systems are entirely different from each other but MPPT utilized the mechanical tracking device. Initially consider the solar panel to know how the MPPT process. The solar panel generates different power outputs, because it contains P-V characteristics which define multiple operating point.

$$I = Is(e^{(Vd/_{nVt})} - 1) \quad (2)$$

$$I = I_{l-I_d} \tag{3}$$

The series and shunt resistance are included in the PV cell model. The internal resistance is Rs and the shunt connected resistance is Rp. From the equation (13) the voltage current characteristics are taken. Figure 2 shows Electrical Equivalent.

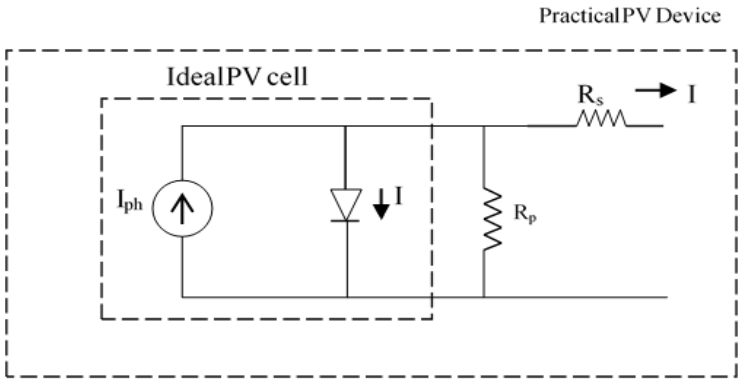

Figure 2 Electrical Equivalent

Ideal photovoltaic cell is modelled such that the diode is placed parallel to the current source. Shunt resistances and series resistances must be connected to the photovoltaic cell model, since no solar cell is ideal which is mentioned in the PV cell.

2.1.1 Representation of PV devices

PV system can be classified into two types such as single and double diode type.

2.1.1.1 *Single Diode Type*

Fig 3 shows that the single diode circuit model of the photovoltaic array system. The shunt resistance is also connected with the diode. But the load resistance is connected series with the shunt resistance.

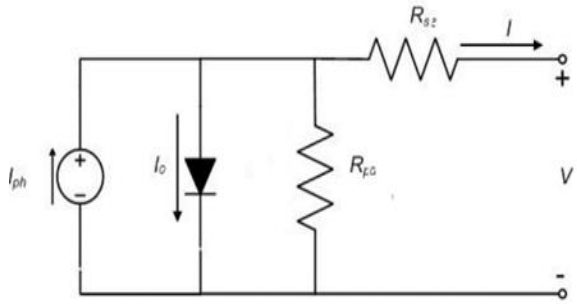

Figure 3 Single Diode type

The loop equation is defined,

$$I = Iph - Io\ [\ \exp\left(\frac{V+RseI}{Vta}\right) -1 - \frac{V+ RseI}{Rpa} \qquad (4)$$

2.1.1.2 *Double Diode Type*

As same as single diode type only difference is, the diode is connected in parallel. The shunt resistance is also connected with the diode(shown in figure 4). But the load resistance is connected series with the shunt resistance.

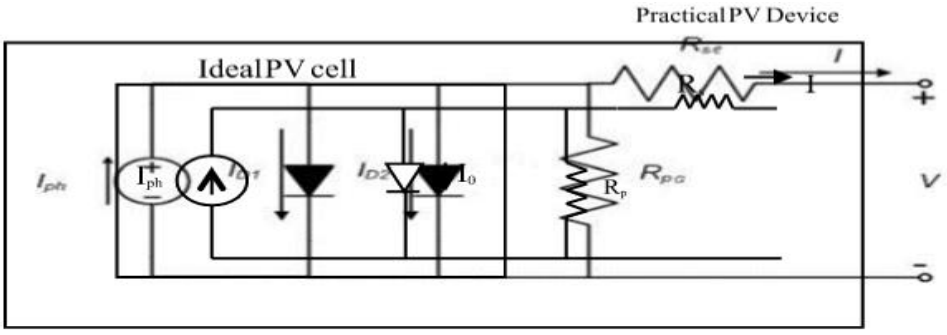

Figure 4 Double Diode Model

General equation of this model can be given below,

$$I = I_{ph} - I_{01}\{\exp\left[\frac{(V+RseI)}{Vt} - 1\right]\} - I_{02}\{\exp\left[\frac{(V+RseI)}{aVt} - 1\right]\} - \frac{(V+RseI)}{Rpa} \quad (5)$$

$$Ios = Ios,n\left(\frac{Tn}{T}\right)^3 \exp\left[\frac{qEg}{ak}\left(\frac{1}{Tn} - \frac{1}{T}\right)\right.$$

Where, Eg is bandgap energy in the semiconductor
And $I_{os,n}$ saturation current of diode , it can be given by

$$I_{os,n} = \frac{Isn}{exp\left(\frac{Von}{aVtn}\right)-1} \quad (6)$$

I_{sn} ,V_{on} and V_{tn} are the current and voltage in short and open circuit.
Modified single diode circuit is given in equation (7)

$$Ios,\ n = \frac{(Isn+Ki\Delta T)}{exp\left[\left(\frac{(Von+Kv\Delta T)}{aVtn}\right)\right]-1} \quad (7)$$

Because of the temperature dependence on saturation current; T. I-V and P-Vfeatures can be easily achieved.

2.2 BLDC Motor

BLDC motors is built in various physical arrangement. In any case, a three-stage PLTC motor with a durable magnetic rotor is the most commonly used. The development of this engine has numerous likenesses of three stage enlistment engine just as traditional DC engine.

The differential equations are given for 3 phase 2-pole BLDC motor the stator will be star-associated concentrated. The hall-effect sensor can be provided with 120° phase shift.

$$V_X = R_X I_X + E_{\Psi X} \quad (8)$$

Where I_{XV_X} is the phase current and voltage. The emf induce can be expressed as,

$$E_{\Psi X} = \frac{d\Psi X}{dt} \quad (9)$$

Consider (Ψ_X) as the Ψ_A, Ψ_B, Ψ_C

For Phase A,B,C flux (Ψ_A, Ψ_B, Ψ_C) is

$$\Psi_A = L_A I_A + M_{AB} I_B + M_{AC} I_C + \Psi_{pm}(\theta) \quad (10)$$

$$\Psi_B = L_B I_B + M_{BC} I_C + M_{BA} I_A + \Psi_{pm}(\theta) \quad (11)$$

$$\Psi_C = L_B I_B + M_{CA} I_A + M_{CB} I_B + \Psi_{pm}(\theta) \quad (12)$$

Where $\Psi_{pm}(\theta)$ represented as permanent magnet flux linkage of 3 phase , $\theta$is the angle of rotor $L_A = L_B = L_C$ is the self inductance, and $M_{AB} = M_{AC} = M_{BC} = M_{BA} = M_{CA} = M_{CB}$represented as mutual inductance.

$$V_A = R_{IA} + \frac{d}{dt}(L_A I_A + M_{AB} I_B + M_{AC} I_C) + E_A \quad (13)$$

Substitute 10 and 11 in 12

$$V_B = R_{IB} + \frac{d}{dt}(L_B I_B + M_{BC} I_C + M_{BA} I_C) + E_B \quad (14)$$

Substitute 8 and 9 in 13

$$V_C = R_{IC} + \frac{d}{dt}(L_C I_C + M_{CA} I_A + M_{CB} I_B) + E_C \quad (15)$$

$$M_{AB} = M_{AC} = M_{BC} = M_{BA} = M_{CA} = M_{CB} = M(\quad (16)$$

$$L_A = L_B = L_C = L \quad (17)$$

$$I_A + I_B + I_C = 0 \quad (18)$$

Substitude (5) in (6)

$$V_A = R_{IA} + L\frac{dI_A}{dt} - M\frac{dI_A}{dt} + E_A \quad (19)$$

Substitude (7) in (8)

$$V_B = R_{IB} + L\frac{dI_B}{dt} - M\frac{dI_B}{dt} + E_B \quad (20)$$

Substitude (11) in (12)

$$V_C = R_{IC} + L\frac{dI_C}{dt} - M\frac{dI_C}{dt} + E_C \quad (21)$$

The rotor angle (θ) in terms of backEMF can be given by

$$E_A = \Psi_m \omega_r f_A(\theta_e) \quad (22)$$

$$E_B = \Psi_m \omega_r f_B\left(\theta_e + \frac{2\pi}{3}\right) \quad (23)$$

$$E_C = \Psi_m \omega_r f_C\left(\theta_e - \frac{2\pi}{3}\right) \quad (24)$$

$$\omega_r = \left(\frac{P}{2}\right)\omega_m \quad (25)$$

Where $\Psi_m$is the utmost eternal magnetflux linkage.

$$E_A = \Psi_m\left(\frac{P}{2}\right)\omega_m f_A(\theta_e) \quad (26)$$

$$Pole \quad pair = \frac{Number \quad of \quad poles(P)}{2} \quad (27)$$

$$E_A = \omega_m\left(\frac{K_b}{2}\right) f_A(\theta_e) \quad (28)$$

$$K_b = P\Psi_m \quad (29)$$

Substitute (29) in (27)

$$E_A = \omega_m\left(\frac{K_b}{2}\right) f_A(\theta_e) \quad (30)$$

$$E_B = \omega_m\left(\frac{K_b}{2}\right) f_A\left(\theta_e + \frac{2\pi}{3}\right) \quad (31)$$

$$E_C = \omega_m\left(\frac{K_b}{2}\right) f_C\left(\theta_e - \frac{2\pi}{3}\right) \quad (32)$$

Where $f_A(\theta_e), f_B(\theta_e), f_C(\theta_e)$are the functions of rotor position. The $f_A(\theta_e), f_B(\theta_e), f_C(\theta_e)$ are mentioned astrapezoidal function, which limit between +1 to-1 are expressed as,

$$f_A(\theta_e) = \begin{cases} \frac{6}{\pi}\theta_e & 0 < \theta_e \leq {}^{\pi}/_{6} \\ -\frac{6}{\pi}\theta_e + 6 & {}^{\pi}/_{6} < \theta_e \leq {}^{5\pi}/_{6} \\ -1 & {}^{7\pi}/_{6} < \theta_e \leq 2\pi/6 \\ -\frac{6}{\pi}\theta_e - 12 & {}^{11\pi}/_{6} < \theta_e \leq 2\pi \end{cases} \quad (33)$$

$$f_B(\theta_e)=\begin{cases}-1 & 0<\theta_e\le {}^{\pi}/_{2}\\ \frac{6}{\pi}\theta_e-4 & {}^{\pi}/_{2}<\theta_e\le {}^{5\pi}/_{6}\\ 1 & {}^{5\pi}/_{6}<\theta_e\le 9\pi/6\\ -\frac{6}{\pi}\theta_e+10 & {}^{9\pi}/_{6}<\theta_e\le 11\pi/6\\ -1 & {}^{11\pi}/_{6}<\theta_e\le 2\pi\end{cases} \quad (34)$$

$$f_B(\theta_e)=\begin{cases}1 & 0<\theta_e\le {}^{\pi}/_{6}\\ -\frac{6}{\pi}\theta_e+4 & {}^{\pi}/_{6}<\theta_e\le {}^{\pi}/_{2}\\ -1 & {}^{\pi}/_{2}<\theta_e\le 7\pi/6\\ \frac{6}{\pi}\theta_e-8 & {}^{7\pi}/_{6}<\theta_e\le 9\pi/6\\ 1 & {}^{9\pi}/_{6}<\theta_e\le 2\pi\end{cases} \quad (35)$$

2.2.1 *Modeling of Motion Equation*

$$T_E=T_A+T_B+T_C \quad (36)$$

$$T_E=\frac{(E_AI_A+E_BI_B+E_CI_C)}{\omega_m} \quad (37)$$

$$T_E=\frac{P\Psi_m}{2}[f_A\left(\theta_e+\frac{2\pi}{3}\right)I_B+f_c\left(\theta_e-\frac{2\pi}{3}\right)I_C \quad (38)$$

These motor works in 120° conduction . TE is given as

$$T_E=\frac{P\Psi_m}{2} \quad (39)$$

$$T_E=K_TI \quad (40)$$

Where K_T is the torque coefficient.
The motion equation is ,

$$T_E-T_L=\int\frac{d\omega_m}{dt}+B\omega_m \quad (41)$$

$$\frac{d\omega_m}{dt}=\frac{1}{J}(T_E-T_L-B\omega_m) \quad (42)$$

$$\omega_m = \int \frac{1}{J}(T_E - T_L - B\omega_m) \quad (43)$$

$$\omega_m = \left(\frac{2}{P}\right)\omega_r \quad (44)$$

$$\omega_r = \left(\frac{d\theta_r}{dt}\right) \quad (45)$$

$$\frac{d\theta_r}{dt} = (\frac{P}{2})\omega_m \quad (46)$$

2.3 Centrifugal Water Pump

It is the commonly used kinetic energy pump and the liquid enters the casing, force pushes liquid outward from the eye of the impeller. By using large impeller or increase the number of impellers the differential head is increased by turning the impeller faster. To reduce the friction of rotation and the movement of the shaft thrust bearing and shaft radial are restricted.

3 Control of Proposed System

3.1 Gray Wolf Optimization

To achieve intelligent algorithm grey wolf population by means of tracking, hunting, encircling, attacking and other processes was used. The Improved GWO algorithm partakes the benefits of guileless code, fewer parameter adjustments, easy implementation and strong global search capability.

To define the distance among the individual and is shown in the equation 47

$$D=|C.\ X_p(t) - X(t)\ | \quad (47)$$

Constant C is the swing factor is shown in the equation 48

$$C=2r_1 \quad (48)$$

Where, r1 is a random number from 0 to 1. In the equation (48), the grey wolf's position updating formula is presented.

$$X(t+1) = X_p(t) - A.D \quad (49)$$

$$A = 2a_2 - a \quad (50)$$

While considering the grey wolf for the simulation of the hunting behavior, think that α wolf, β wolf and δ wolf has a superior comprehension to the area of the prey, therefore area of the prey can be controlled by utilizing the area of the grey wolf population. The leader wolf α, commands β and δ to hunt as soon as they receive the positional information of the pray. Updating the positional information such as α, β and δ wolf is carried out in the grey wolf population.

$$D_\alpha = |C_1 . X_\alpha(t) - X(t) \quad (51)$$

$$D_\beta = |C_2 . X_\beta(t) - X(t)| \quad (52)$$

$$D_\delta = |C_3 . X_\delta(t) - X(t)| \quad (53)$$

$$X_1 = X_\alpha - A_1 . D_\alpha \quad (54)$$

$$X_2 = X_\beta - A_2 . D_\beta \quad (55)$$

$$X_3 = X_\delta - A_3 . D_\delta \quad (56)$$

$$X_p(t+1) = \frac{X_1 + X_2 + X_3}{3} \quad (57)$$

4 Result and Discussion

By using MATLAB/Simulink can be provide the result for solar PV system. This section provides the more comparison study of optimization techniques. The Simulink model can be shown in Figure 5,

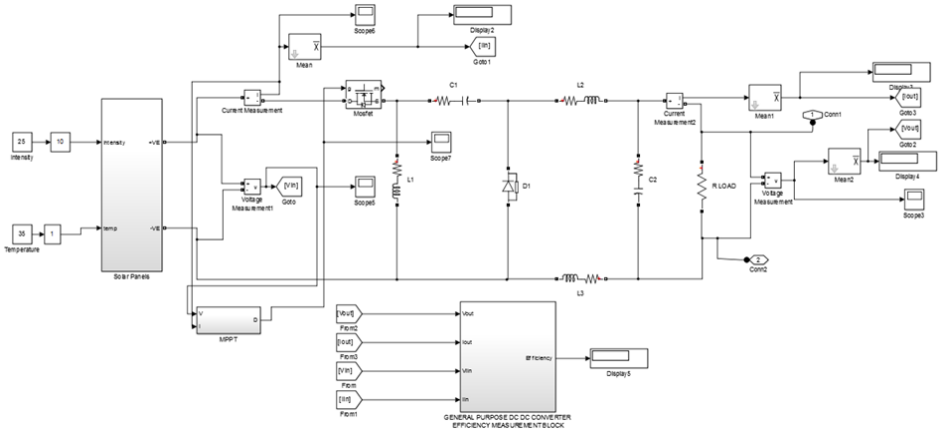

Figure 5 Simulation diagram of Luo Converter

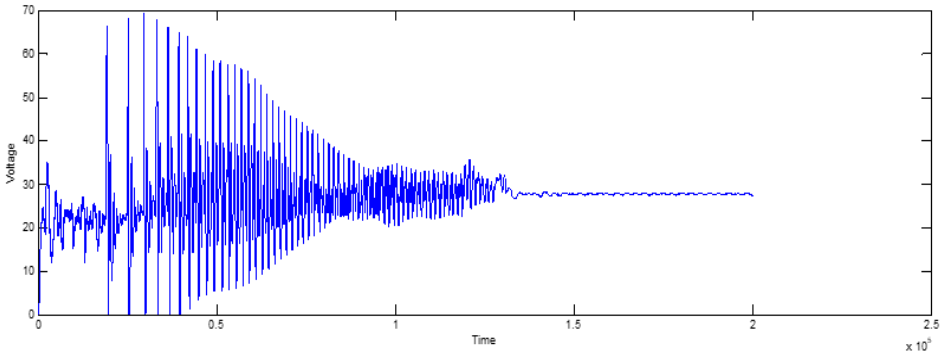

Figure 6 simulation result of Luo Converter

From figure 6 indicated the luo converter with time in x axis and voltage in y axis. The converter is mainly used to convert DC to DC voltage.

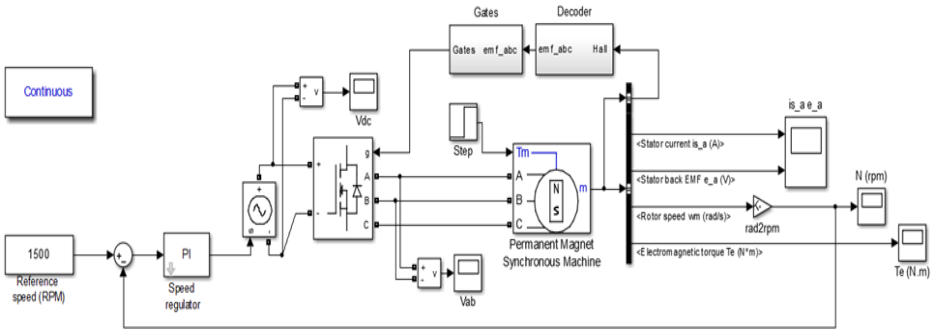

Figure 7 BLDC motor for electromagnetic torque ripples

Figure 7 shows the simulation diagram of BLDC motor. It is to reduce the electromagnetic DC motor. The back emf cuts the magnetic flux and opposes the current flowing through the conductor. The starting value of the back emf is zero and the values depend upon the speed of rotation of the armature conductor. Figure 8 shows Current and back emf of BLDC motor to reduce torque. Figure 9 shows Speed response of BLDC motor to reduce torque. Figure 10 shows Torque waveform of BLDC motor to reduce ripples

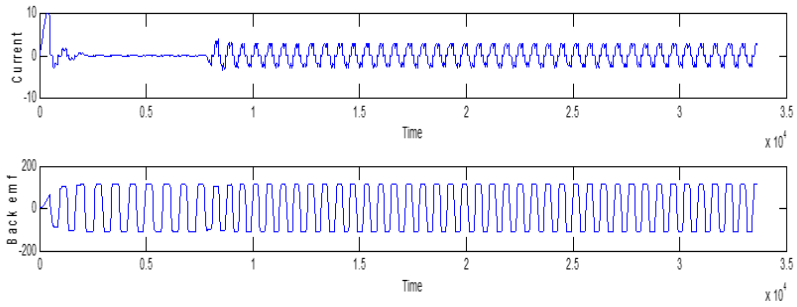

Figure 8 Current and back emf of BLDC motor to reduce torque

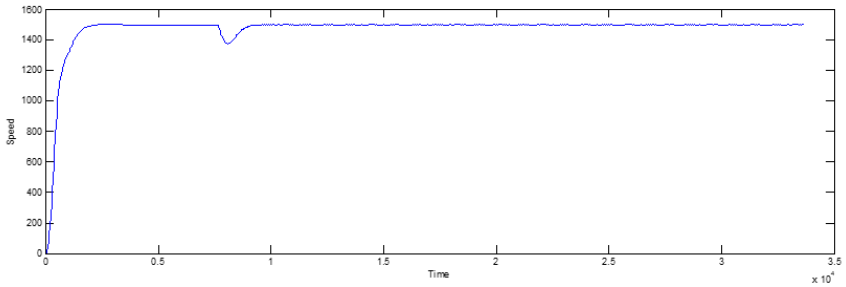

Figure 9 Speed response of BLDC motor to reduce torque

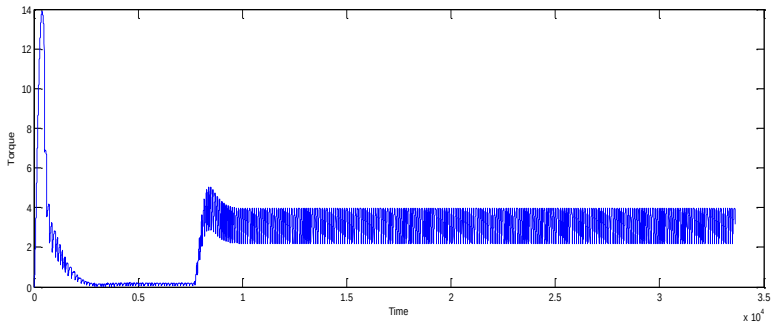

Figure 10 Torque waveform of BLDC motor to reduce ripples

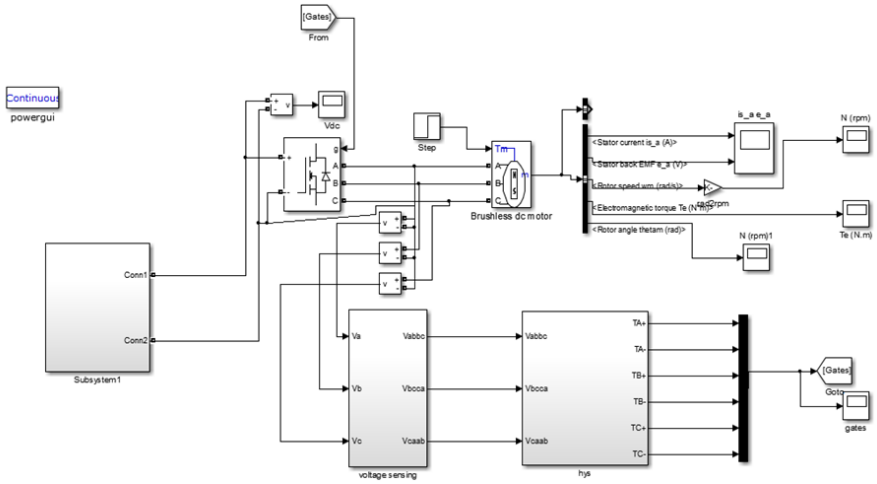

Figure 11 Simulation diagram of open loop Permanent Magnet Brushless DC motor

Open-loop control systems are very simple in construction, stable and low cost. But this system does not track the output of the controlling

process. Figure 11 shows the Simulation block diagram of open-loop speed control DC motor.

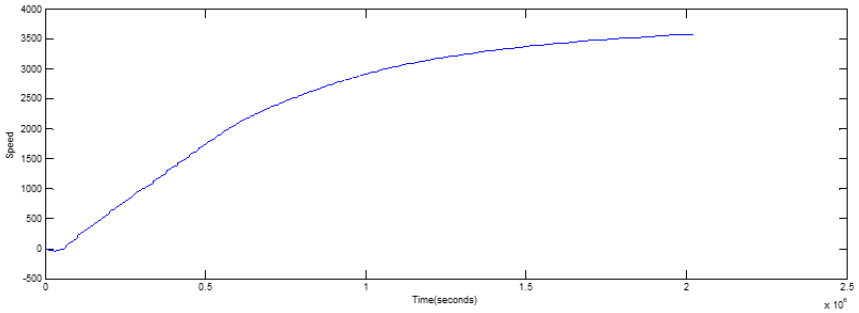

Figure 12 Speed response of BLDC motor

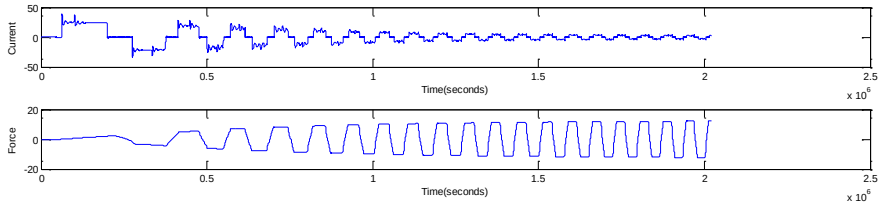

Figure 13 Current waveform of BLDC motor

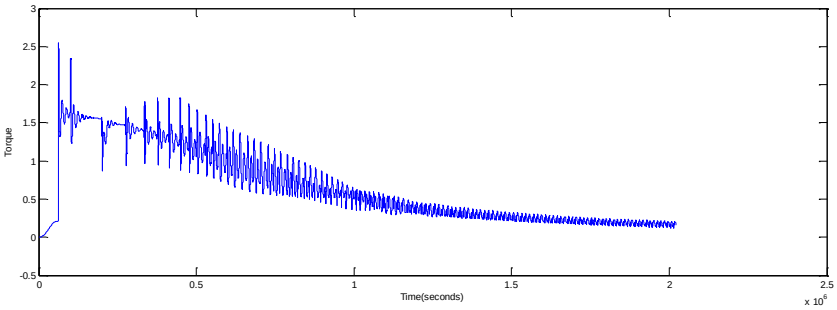

Figure 14 Torque waveform of BLDC motor

Figure 12 indicates Permanent Magnet open loop control. Here even though the speed settles fast, unfortunately the overshoot is very high and the oscillations present in the initial stage continue throughout the operation controlled in open-loop system.

A figure 13 and 14 represents the open loop current and torque r. The simulation result shows the current and torque waveform operating for open loop which has oscillations over the whole range.

Table 1 BLDC Motor parameters

Variables	Value
Torque range	6.4 Nm
Power	250 W
Speed value	380 rpm
High voltage	48 V
Low current	5.2 A

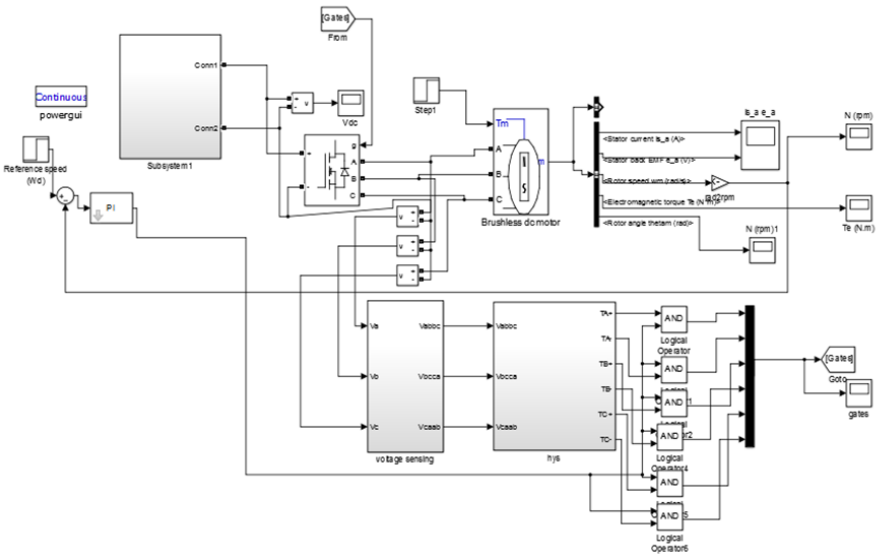

Figure 15 Simulation diagram of closed loop

BLDC machines are widely used in closed-loop control systems because of their excellent control properties and fast response. In closed-loop speed control, the controlled variable (speed) sensed at every instant of

time, feedback and compared with the reference speed resulting in an error signal. Figure 15 shows Simulation diagram of closed loop

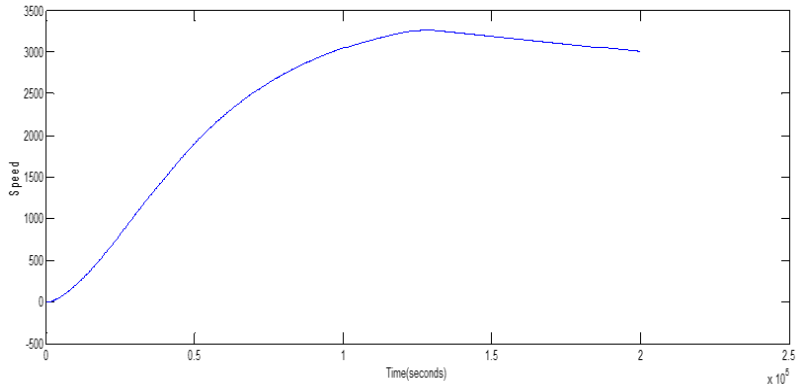

Figure 16 Speed response of BLDC motor with closed loop

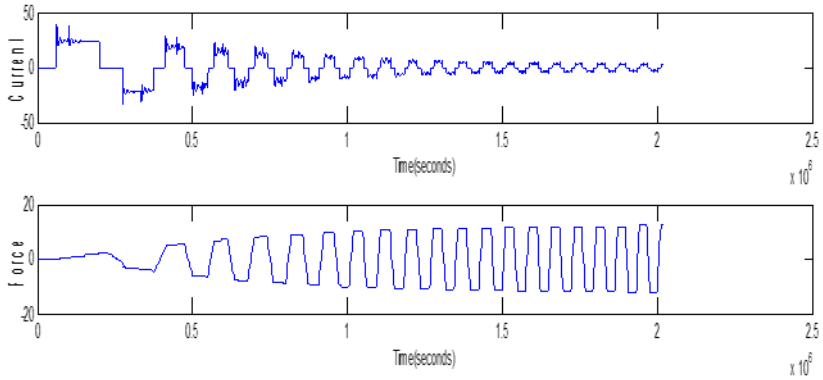

Figure 17 Current and electromagnetic force waveform of BLDC motor with closed loop

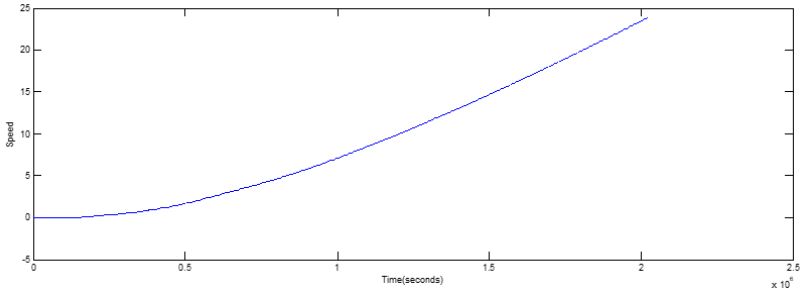

Figure 18 Torque waveform of BLDC motor

Figure 16 indicates of Permanent Magnet closed loop control. Here the over shoot is low. The simulation result shows the current and torque waveform operating for closed loop which has oscillations over the whole range.

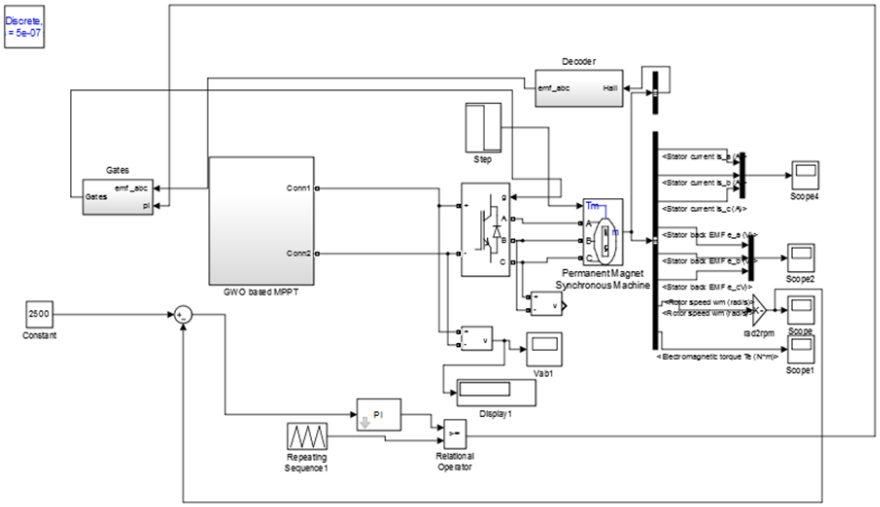

Figure 19 Simulink model of the proposed system

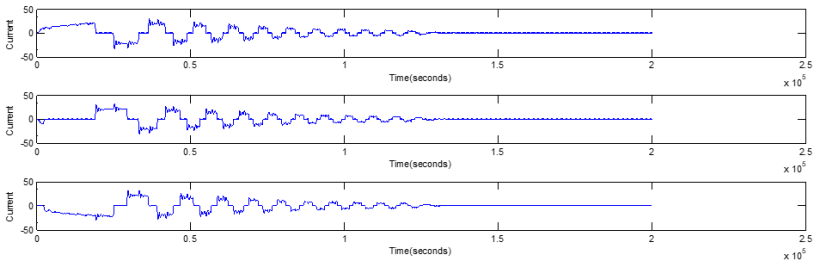

Figure 20 Current waveform of solar PV fed BLDC motor with closed loop system

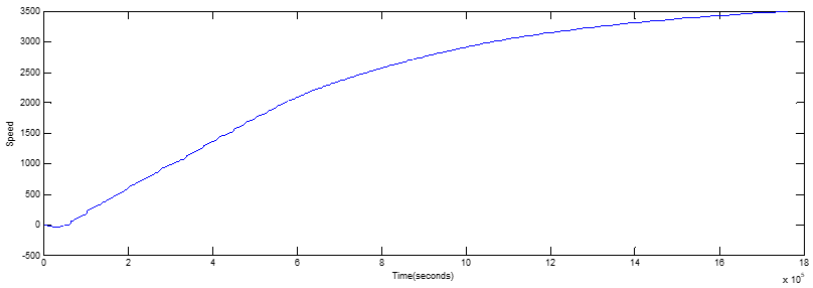

Figure 21 Speed response of solar PV fed BLDC motor with closed loop system

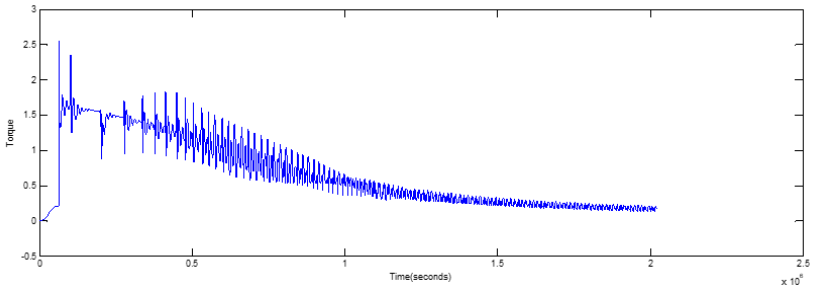

Figure 22 Torque waveform of solar PV fed BLDC motor with closed loop system

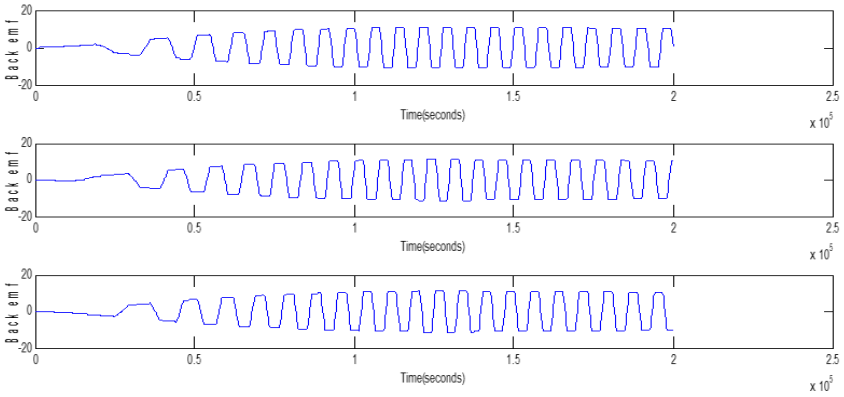

Figure 23 Back emf waveform of solar PV fed BLDC motor with closed loop system

The comparison table of MPPT is given Table 2.The time response of settling time of voltage in GWO based MPPT is better than P&O, INC MPPT. The Settling time of GWO based MPPT is low compared the P&O and INC MPPT. Comparison of time domain specification indicates in table 3. In this Table 3 the result of GWO is better in both rise time and settling time compared to the other. Table 4 shows Steady state performance result

Table 2 Comparison table of MPPT

MPPT technique	**Output Power(W)**	**Efficiency (%)**
Incremental Conductance	400.34	86
Perturb and Observe	455	89
GWO	490	91

Table 3 Time domain Specification of PV fed Luo Converter

Different MPPT techniques	**Time Domain Specifications**	
	Settling time (Sec)	**Rise time (Sec)**
Incremental Conductance	0.02	0.008
P&O	0.01	0.008
GWO	0.008	0.003

Figure 17 shows Current and electromagnetic force waveform of BLDC motor with closed loop. Figure 18 Torque waveform of BLDC motor. Figure 19 shows Simulink model of the proposed system. Figure 20 shows Current waveform of solar PV fed BLDC motor with closed loop system. Figure 21 shows Speed response of solar PV fed BLDC motor with closed loop system. Figure 22 shows Torque waveform of solar PV fed BLDC motor with closed loop system. Figure 23 shows Back emf waveform of solar PV fed BLDC motor with closed loop system

Table 4 Steady state performance result

Source Voltage(V)	**Perturb and Observe** efficiency (%)	**Incremental Conductance** efficiency (%)	**GWO** efficiency (%)
200	90.1	90.1	90.1
	91.8	88.4	88.4
	91.8	91.8	88.4
220	92.23	93.08	93.08
	94.78	8.28	92.23
	93.93	93.5	92.23
240	93.69	93.93	93.69
	94.63	89.72	93.31
	89.16	91.61	93.12

The efficiencies of the three algorithms were plotted against the Source voltage shown in fig 24. From this we have concluded that the GWO was the best in terms of steady state performance, followed by INC and P&O.

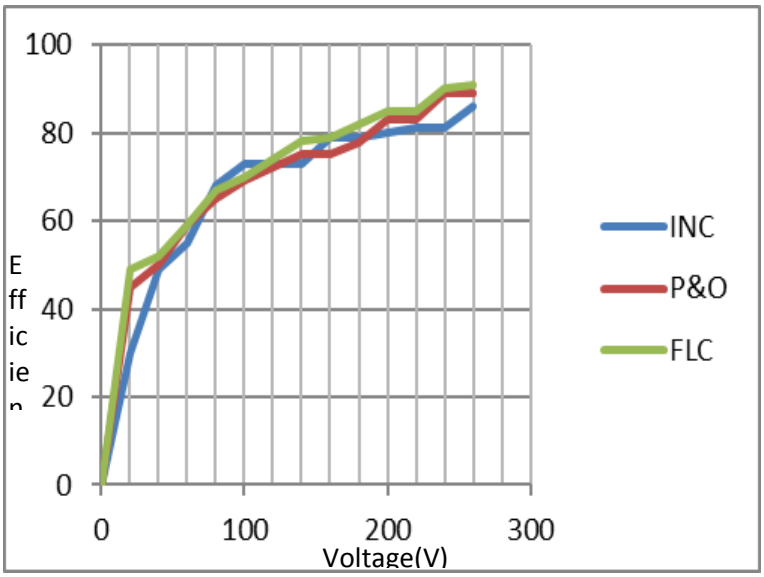

Figure 24 Efficiency vs. source voltage

5 Conclusion

A Grey Wolf Optimization algorithm is introduced for the speed control system by using converter. The proposed method is simulated and modeled by using MATLAB/SIMULINK and sim power system tool boxes. Simulation results proved the suitability of the proposed method. In order to reduce the stress on power devices luo converter is operated. By comparing the simulation result with other optimization technique, the proposed method outperforms the other method.

References

[1] Zhou Xuesong,Song Daichun, Ma Youjie, Cheng Deshu," The simulation and design for MPPT of PV system Based on Incremental Conductance Method", WASE International Conference on Information Engineering ,2010.

[2] Bidyadhar Subudhi, Raseswari Pradhan," A Comparative Study on Maximum Power Point Tracking Techniques for Photovoltaic Power

Systems", IEEE Transactions on Sustainable Energy, Vol. 4, No. 1, pp.89-98, 2013.

[3] Bhim Singh , Vashist Bist," Power quality improvements in power factor correction Luo converter fed brushless direct current motor drive", International Transactions on Electrical Energy Systems, Vol.25, No.5, pp.898-919, 2015.

[4] Bhim Singh, Vashist Bist, Ambrish Chandra, Kamal AI-Haddad," Power Quality Improvement in PFC Bridgeless-Luo Converter Fed BLDC Motor Drive",IEEE Industry Application Society, 2013.

[5] Dylan D.C. Lu, Quang Ngoc Nguyen," A photovoltaic panel emulator using a buck-boost DC/DC converter and a low cost micro-controller",Solar Energy,Vol.86,No.5,pp.1477-1484, 2012.

[6] Sachin Jain, T. Athiesh Kumar, Ramsha Karampuri, , V. T. Somasekhar," A Single-Stage PhotoVoltaic System for a Dual- Inverter fed Open-End Winding Induction Motor Drive for Pumping Applications",IEEE Transactions on Power Electronics,Vol.30,No.9,pp.4809-4818, 2015.

[7] Le An, Dylan Dah-Chuan Lu," Design of a Single-Switch DC/DC Converter for a PV-Battery Powered Pump System with PFM+PWM Control ", IEEE Transactions on Industrial Electronics, Vol.62, No.2, pp.910-921, 2015.

[8] João Victor Mapurunga Caracas, Guilherme de Carvalho Freitas,Luis Felipe Moreira Teixeira, Luiz Antonio de Souza Ribeiro," Implementation of a High Efficiency, High Lifetime, and Low Cost Converter for an Autonomous Photovoltaic Water Pumping System",IEEE Transcactions on Industry Applications,Vol.50,No.1,pp.631-641, 2014.

[9] Mahdi Ouada, Mohamed Salah Meridjet, Nabil Taibi," Optimization photovoltaic pumping system based BLDC using Fuzzy logic MPPT control", International Renewable and Sustainable Energy Conference (IRSEC) ,2013.

[10] Shiqing Tang et al ," An Enhanced MPPT Method Combining Fractional-Order and Fuzzy Logic Control", IEEE Journal of Photovoltaics, Vol.7, No.2, pp.640-650, 2017.

[11] Satyajit Mohanty, Bidyadhar Subudhi, Pravat Kumar Ray," A Grey Wolf Assisted Perturb & Observe MPPT Algorithm for a PV System", IEEE Transactions on Energy Conversion, Vol.32, No.1, pp.340-347, 2017.

[12] Nishant Kumar, Ikhlaq Hussain, Bhim Singh, Bijaya Ketan Panigrahi," Single Sensor based MPPT of Partially Shaded PV System for Battery Charging by using Cauchy and Gaussian Sine Cosine Optimization", IEEE Transactions on Energy Conversion, Vol.32, No.3, pp.983-992, 2017.

[13] Satyajit Mohanty, Bidyadhar Subudhi, Pravat Kumar Ray," A New MPPT Design Using Grey Wolf Optimization Technique for Photovoltaic System Under Partial Shading Conditions", IEEE Transactions on Sustainable Energy, Vol.7, No.1, pp.181-188, 2016.

[14] Alivarani Mohapatra, Byamakesh Nayak, Priti Das, Kanungo Barada Mohanty," A review on MPPT techniques of PV system under partial shading condition", Renewable and Sustainable Energy Reviews, Vol.80, pp.854-867, 2017.

[15] T.R. Premila," Solar PV Array Fed BLDC Motor using DC-DC Converter", International Journal of Control Theory and Applications, Vol.10, No.25, pp.43-54, 2017.

[16] Bhim Singh, Rajan Kumar," Solar photovoltaic array fed water pump driven by brushless DC motor using Landsman converter", IET Renewable Power Generation, Vol.10, No.4, pp.474-484, 2016.

Biographies

Rana Adil Abdul-Nabe received a B.Sc degree in Mechanical Engineering (with honors) from Technical College AL-Mussaib, Babil, Iraq in 2005. received an M.Sc. degree in Mechanical Engineering Sam Higgin bottom Institute of Agriculture, Technology & Sciences, India in 2014. Main research interests in solar power systems and Hydraulic pumps in electric power plants, she has two international publications in the Mechanical Engineering Sciences. work as an assistant lecturer at Al-Furat Al-Awsat Technical University, Babil, Iraq.

Rawaa A. Abdul –Nabi received a B.Sc degree in Physical Sciences (with honors) from the University of Babylon, Babil, Iraq in 2007. She received an M.Sc. degree in Physics from the University of Babylon Babil, Iraq in 2016. Main research interests in Electron – Nucleus Scattering Form Factors of Some Light Nuclei Using Large Scale Shell Model, she has two international publications in the Physical Sciences, one international publication in laser technology application. work as an assistant lecturer at Al-Furat Al-Awsat Technical University, Babil, Iraq.

Sara Al-waisawy was born in Babylon, Iraq. She received her Bachelor's degree in Electrical Engineering from Babylon University, Iraq in 2009 and her master's degree in Electrical Engineering and computer science from Ohio University, united states of America in 2014. Her main research interests are in the Electronic field and Optoelectronics and Photonics area. She has 4 international publications in the Electronic and Luminescence. She is currently working as Assistant Lecturer with AL-Mussaib Technical College, AL-Furat Al-Awsat Technical University, Iraq.